

****Volume Title****

*ASP Conference Series, Vol. **Volume Number***

****Author****

© ****Copyright Year**** *Astronomical Society of the Pacific*

An ADER-WENO Finite Volume AMR code for Astrophysics

O. Zanotti¹, M. Dumbser¹, A. Hidalgo² and D. Balsara³

¹*Laboratory of Applied Mathematics, Department of Civil, Environmental and Mechanical Engineering, University of Trento, Via Mesiano 77, I-38123 Trento, Italy*

²*Departamento de Matemática Aplicada y Métodos Informáticos, Universidad Politécnica de Madrid, Calle Ríos Rosas 21, E-28003 Madrid, Spain*

³*Physics Department, University of Notre Dame du Lac, 225 Nieuwland Science Hall, Notre Dame, IN 46556, USA*

Abstract. A high order one-step ADER-WENO finite volume scheme with Adaptive Mesh Refinement (AMR) in multiple space dimensions is presented. A high order one-step time discretization is achieved using a local space-time discontinuous Galerkin predictor method, while a high order spatial accuracy is obtained through a WENO reconstruction. Thanks to the one-step nature of the underlying scheme, the resulting algorithm can be efficiently imported within an AMR framework on space-time adaptive meshes. We provide convincing evidence that the presented high order AMR scheme behaves better than traditional second order AMR methods. Tests are shown of the new scheme for nonlinear systems of hyperbolic conservation laws, including the classical Euler equations and the equations of ideal magnetohydrodynamics. The proposed scheme is likely to become a useful tool in several astrophysical scenarios.

1. Introduction

ADER schemes were introduced more than ten years ago by Toro et al. (2001)¹. Though presenting several attractive features, like the possibility of reaching an arbitrary high order of accuracy and the fact that the time update is performed through a single step with no need for Runge-Kutta, in their original form they have never been applied to astrophysics. The reason for this is that original ADER schemes required resorting to the so-called Cauchy-Kovalevski procedure, that is based on a repeated use of the governing conservation laws in differential form. In spite of being conceptually clear, such a procedure becomes rather cumbersome in multiple space dimensions for the classical Euler equations. It has been implemented by Toro & Titarev (2005) and Dumbser et al. (2007), but a wider use has not been reached.

A fundamental breakthrough was achieved by Dumbser et al. (2008), who proposed a variant of the ADER approach in which the local time evolution of the reconstructed polynomials is obtained through an element-local space-time Galerkin predictor that is based on the weak integral form of the PDEs. This new strategy, which

¹See also the subsequent works by Titarev & Toro (2005); Toro & Titarev (2005).

promoted ADER methods to the wider public, has been proved to be rather successful even in the solution of systems of equations with stiff source terms, and has been applied to a variety of specific physical problems (Dumbser & Zanotti 2009; Hidalgo & Dumbser 2011; Zanotti & Dumbser 2011).

The ADER property of performing the time-update through a single step makes them particularly suitable for incorporating adaptive mesh refinement (AMR). This combination is the subject of our work, which describes a new tool for performing high-order numerical calculations on adaptive grids. We refer to Dumbser et al. (2013) for more details about the new approach, and to Dumbser et al. (2014) for the application of the same ideas to non-conservative hyperbolic systems.

2. The numerical scheme

The partial differential equations under consideration are of the type

$$\frac{\partial \mathbf{u}}{\partial t} + \frac{\partial \mathbf{f}}{\partial x} + \frac{\partial \mathbf{g}}{\partial y} + \frac{\partial \mathbf{h}}{\partial z} = \mathbf{S}(\mathbf{u}, \mathbf{x}, t), \quad (1)$$

where \mathbf{u} is the vector of conserved quantities, while $\mathbf{f}(\mathbf{u})$, $\mathbf{g}(\mathbf{u})$ and $\mathbf{h}(\mathbf{u})$ are the fluxes. According to the finite volume approach, the time update is performed through the standard discretization

$$\begin{aligned} \bar{\mathbf{u}}_{ijk}^{n+1} = & \bar{\mathbf{u}}_{ijk}^n - \frac{\Delta t}{\Delta x_i} \left(\mathbf{f}_{i+\frac{1}{2},jk} - \mathbf{f}_{i-\frac{1}{2},jk} \right) - \frac{\Delta t}{\Delta y_j} \left(\mathbf{g}_{i,j+\frac{1}{2},k} - \mathbf{g}_{i,j-\frac{1}{2},k} \right) \\ & - \frac{\Delta t}{\Delta z_k} \left(\mathbf{h}_{i,j,k+\frac{1}{2}} - \mathbf{h}_{i,j,k-\frac{1}{2}} \right) + \Delta t \bar{\mathbf{S}}_{ijk}. \end{aligned} \quad (2)$$

In a nutshell, the modern ADER strategy provides an implementation of Eq. (2) through the following three steps

- **High order reconstruction.** This is performed through WENO schemes, in which the sought reconstructed polynomial is written in terms of a nodal basis $\psi_p(\xi)$ of polynomials of degree M . In one spatial dimension, say x , this corresponds to the expansion

$$\mathbf{w}_h^{s,x}(x, t^n) = \sum_{p=0}^M \psi_p(\xi) \hat{\mathbf{w}}_{ijk,p}^{n,s}, \quad (3)$$

where $\xi \in [0, 1]$ is the reference coordinate defined by $x = x_{i-1/2} + \xi \Delta x_i$, $\hat{\mathbf{w}}_{ijk,p}^{n,s}$ are unknown coefficients to be determined, while the index s refers to the stencil for which reconstruction is performed [see Dumbser et al. (2008) for more details].

- **Local Predictor in time.** Once a high order polynomial in space \mathbf{w}_h has been reconstructed for each cell, it is necessary to evolve it in time in order to compute the fluxes while preserving the order of accuracy. This is obtained after writing a local weak form of the governing equations, namely

$$\int_0^1 \int_0^1 \int_0^1 \int_0^1 \theta_q \left(\frac{\partial \mathbf{u}}{\partial \tau} + \frac{\partial \mathbf{f}^*}{\partial \xi} + \frac{\partial \mathbf{g}^*}{\partial \eta} + \frac{\partial \mathbf{h}^*}{\partial \zeta} - \mathbf{S}^* \right) d\xi d\eta d\zeta d\tau = 0, \quad (4)$$

where the θ_p are given by a tensor-product of the basis functions ψ_p already used in the reconstruction procedure, while

$$\mathbf{f}^* = \frac{\Delta t}{\Delta x_i} \mathbf{f}, \quad \mathbf{g}^* = \frac{\Delta t}{\Delta y_j} \mathbf{g}, \quad \mathbf{h}^* = \frac{\Delta t}{\Delta z_k} \mathbf{h}, \quad \mathbf{S}^* = \Delta t \mathbf{S}. \quad (5)$$

are the fluxes and sources over the reference coordinates. After integration by parts in time, Eq. (4) leads to the solution of a local nonlinear system of equations in the unknowns degrees of freedom of the reconstructed polynomials.

- **Time update.** This is essentially obtained through the scheme (2), in which the fluxes can be computed with a high order of accuracy, using the information obtained from the local predictor.

3. Adaptive Mesh Refinement

Adaptive mesh refinement has been implemented according to a “cell-by-cell” approach involving a tree-type data structure, which is similar to that of Khokhlov (1998). An arbitrary number of levels of refinement ℓ and of the refinement factor τ can in principle be used, where

$$\Delta x_\ell = \tau \Delta x_{\ell+1} \quad \Delta y_\ell = \tau \Delta y_{\ell+1} \quad \Delta z_\ell = \tau \Delta z_{\ell+1}. \quad (6)$$

In practice, we have typically used $\ell_{\max} = 2$ and $\tau = 3$. The computation of numerical fluxes between two adjacent cells on different levels of refinement is rather straightforward thanks to the use of the local space-time predictor, which computes the predictor solution for each element after reconstruction and which is valid from time t_ℓ^n to time t_ℓ^{n+1} . We emphasize that local time-stepping is naturally obtained, implying a total amount of τ^ℓ sub-timesteps on each level to be performed, in order to reach the time t_0^{n+1} of the coarsest level.

4. Results

We have validated our scheme through a large set of test problems in all spatial dimensions, by solving the classical hydrodynamics and magnetohydrodynamics equations. A limited sample of such tests is reported here.

Figure 1 shows the result of the *forward facing step* problem by Woodward & Colella (1984), which has been solved twice, once at the third order of accuracy and once at the second order, while using the same numerical grid. The grid on the coarsest level is formed by 150×50 control volumes, with $\tau = 4$ and $\ell_{\max} = 2$. The top panel shows the refined grid at time $t = 2.5$; the central panel refers to the third-order ADER-WENO computation, while the bottom panel refers to the second order computation. This indicates that even in the context of space-time adaptive mesh refinement, the use of higher order schemes can become crucial to highlight the formation of small-scale turbulent structures.

Figure 2 shows the distribution of the pressure in the classical *vortex system* of Orszag & Tang (1979), with initial conditions given by

$$(\rho, u, v, p, B_x, B_y) = (\gamma^2, -\sin(y), \sin(x), \gamma, -\sqrt{4\pi} \sin(y), \sqrt{4\pi} \sin(2x)), \quad (7)$$

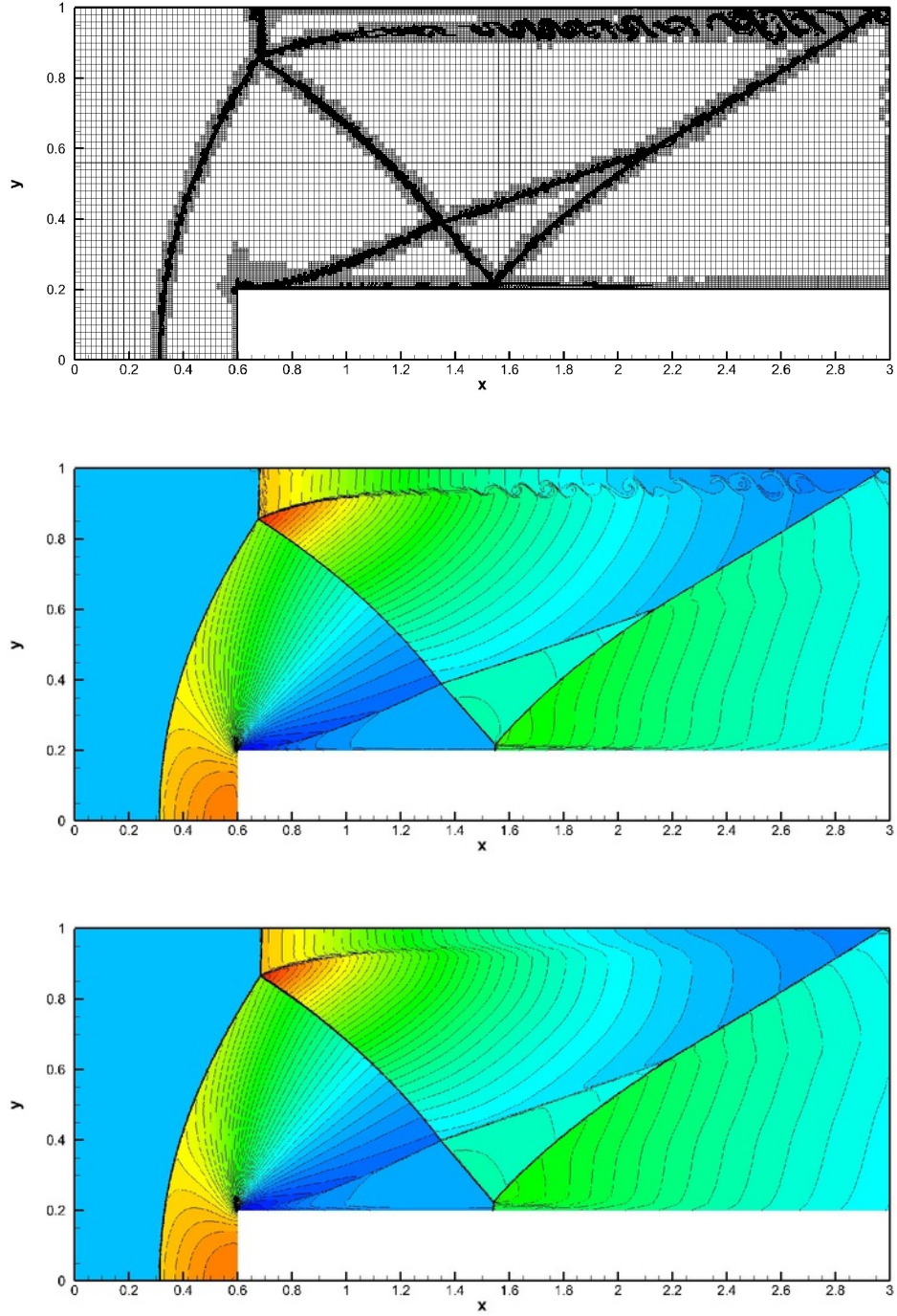


Figure 1. Forward facing step problem. Top panel: AMR grid. Central panel: density contours obtained with the third order ADER-WENO scheme, at time $t = 2.5$. Bottom panel: density contours obtained with the second order ADER-WENO scheme. Reproduced with courtesy from Journal of Computational Physics, Dumbser et al. (2013).

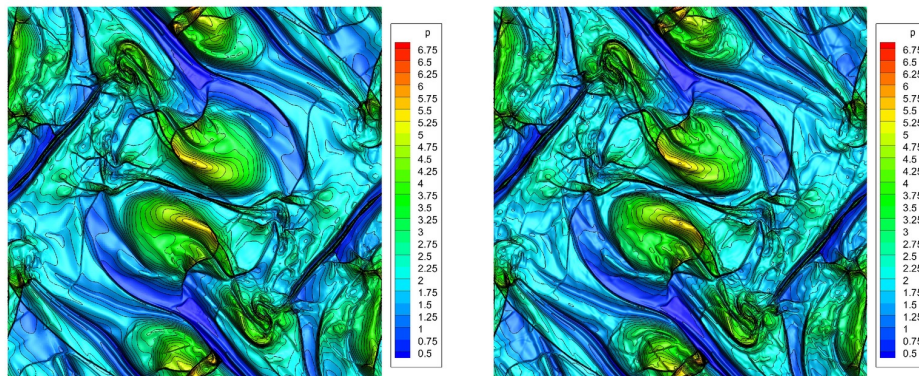


Figure 2. Orszag-Tang vortex system at time $t = 5.0$. Third order ADER-WENO solution obtained on the AMR grid (left) and on a fine uniform grid corresponding to the finest AMR grid level (right). Reproduced with courtesy from Journal of Computational Physics, Dumbser et al. (2013).

where $B_z = 0$ and $\gamma = 5/3$. The AMR computation is reported in the central panel, while the right panel shows a computation obtained on a fine uniform grid that corresponds to the finest AMR grid level. The agreement between the two is excellent, but the AMR simulation, even for such a test where most of the cells are refined, guarantees a speedup of a factor of 1.8 compared to the uniform fine mesh simulation.

Figure 3 shows the distribution of the magnetic pressure in the *MHD rotor problem* in which a rapidly rotating high density fluid is embedded in low density fluid at rest (Balsara & Spicer 1999). On the level zero, the mesh contains 60×60 elements, with $\tau = 4$ and $\ell_{\max} = 2$. Again, the AMR computation is reported on the left, while the right panel reports the result obtained with a fine uniform grid corresponding to the finest AMR grid level. In this case, the benefit of the AMR strategy is particularly evident: while at the final time the AMR grid has only 179680 elements, the uniform fine grid has 921600 elements. This has a strong impact on the CPU time needed for performing the computation, which is a factor 0.14 smaller when the AMR method is adopted.

5. Conclusions

We have described the implementation of ADER-WENO methods with AMR techniques. This combination is rather natural within the ADER approach, which allows for numerical schemes with a single step for the time-update. By providing high order of accuracy both in space and in time, the new scheme is likely to give a significant contribution to the study of delicate astrophysical problems such as turbulence and fluid instabilities, which will be the subject of future research.

References

Balsara, D., & Spicer, D. 1999, Journal of Computational Physics, 149, 270

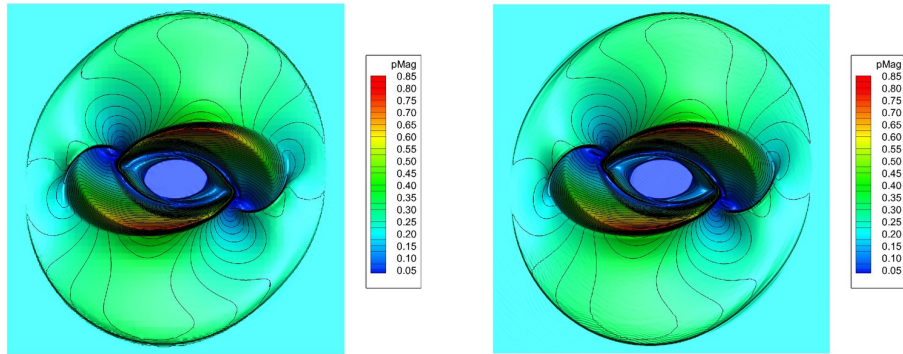


Figure 3. Magnetic pressure in the MHD rotor problem at time $t = 0.25$. Third order ADER-WENO solution obtained on the AMR grid (left) and on a fine uniform grid corresponding to the finest AMR grid level (right). Reproduced with courtesy from Journal of Computational Physics, Dumbser et al. (2013).

- Dumbser, M., Enaux, C., & Toro, E. 2008, Journal of Computational Physics, 227, 3971
- Dumbser, M., Hidalgo, A., & Zanotti, O. 2014, Computer Methods in Applied Mechanics and Engineering, 268, 359-387
- Dumbser, M., Käser, M., Titarev, V., & Toro, E. 2007, Journal of Computational Physics, 226, 204
- Dumbser, M., & Zanotti, O. 2009, Journal of Computational Physics, 228, 6991
- Dumbser, M., Zanotti, O., Hidalgo, A., & Balsara, D. S. 2013, Journal of Computational Physics, 248, 257
- Hidalgo, A., & Dumbser, M. 2011, Journal of Scientific Computing, 48, 173
- Khokhlov, A. 1998, Journal of Computational Physics, 143, 519
- Orszag, S. A., & Tang, C. M. 1979, Journal of Fluid Mechanics, 90, 129
- Titarev, V., & Toro, E. 2005, Journal of Computational Physics, 204, 715
- Toro, E., Millington, R., & Nejad, L. 2001, in Godunov Methods. Theory and Applications, edited by E. Toro (Kluwer/Plenum Academic Publishers), 905–938
- Toro, E., & Titarev, V. 2005, Journal of Computational Physics, 202, 196
- Toro, E. F., & Titarev, V. A. 2005, Journal of Computational Physics, 202, 196
- Woodward, P., & Colella, P. 1984, Journal of Computational Physics, 54, 115
- Zanotti, O., & Dumbser, M. 2011, Monthly Notices of the Royal Astronomical Society, 418, 1004